Gold-assembled silica-coated cobalt nanoparticles as efficient magnetic separation units and surface-enhanced Raman scattering substrate

Lütfiye Sezen YILDIRIM[1] , **Murat KAYA**[2,*] , **Mürvet VOLKAN**[1]
[1]Department of Chemistry, Graduate School of Natural and Applied Science, Middle East Technical University,
Ankara, Turkey
[2]Department of Chemical Engineering and Applied Chemistry, Faculty of Engineering, Atılım University,
Ankara, Turkey

Abstract: Magnetic and optical bifunctional nanoparticles that combine easy separation, preconcentration, and efficient SERS capabilities have been fabricated with high sensitivity and reproducibility through a low-cost method. These gold nanoparticles attached on magnetic silica-coated cobalt nanospheres ($Co@SiO_2/AuNPs$) display the advantage of strong resonance absorption due to gaps at nanoscale between neighboring metal nanoparticles bringing large field enhancements, known as "hot spots". The prepared particles can be controlled by using an external magnetic field, which makes them very promising candidates in biological applications and Raman spectroscopic analysis of dissolved organic species. The magnetic property of the prepared particles lowers the detection limits through preconcentration with solid-phase extraction in SERS analysis. The performance of the prepared nanostructures was evaluated as a SERS substrate using brilliant cresyl blue (BCB) and rhodamine 6G (R6G) as model compounds. The solid-phase affinity extraction of 4-mercapto benzoic acid (4-MBA) using bifunctional $Co@SiO_2/AuNPs$ nanoparticles followed by magnetic separation and the measurement of the SERS signal on the same magnetic particles without elution were investigated. Approximately 50-fold increase in SERS intensity was achieved through solid-phase extraction of 8.3×10^{-6} M 4-MBA in 10 min.

Key words: Bifunctional nanoparticles, core-shell nanoparticles, surface modification, magnetic separation, preconcentration, surface enhanced Raman scattering

1. Introduction

Hybrid nanostructures that contain more than one nanoparticle can display multifunctional properties for applications that are difficult to achieve from single-component nanoparticles.[1−3] Among them, plasmonic-magnetic nanoparticles show both optical properties and magnetic responses.[4] Such multifunctional hybrid nanoparticles are expected to be useful in various fields such as in magnetic/optical dual-modal imaging,[5] drug delivery,[6] and catalysis and biomedicine.[7,8] Another well-known area for the application of plasmonic-magnetic nanoparticles is surface-enhanced Raman scattering (SERS).[9,10]

SERS is known as a technique that is very sensitive to the surface where Raman scattering of adsorbed molecules is enhanced due to the large electric fields associated with surface plasmon resonances generated on rough metal surfaces such as silver, gold, and copper.[11] Colloidal nanoparticles and thin films of gold and silver

---

*Correspondence: muratkaya@atilim.edu.tr

produced with chemical and physical methods are widely used as efficient SERS substrates.[12] Among them, special interest is given to metal nanoparticles due to their large surface area and easy dispersion in liquids. Control over the composition, shape, size, and local environment surrounding the substrate is necessary for monitoring the plasmonic property of these metallic particles.[13−15]

An additional property of the surface plasmon resonance that can be regulated is its dependence on interparticle interactions. This process is known as plasmon coupling and requires the assembly or aggregation of metal nanoparticles into a close-packed structure. Gaps in the nano region between neighboring metallic nanoparticles result in unusually huge field enhancements, known as "hot spots", after laser irradiation.[16,17] Besides, nanoparticles can be assembled and bound onto functionalized planar substrates, which can be used as a SERS substrate.[18,19] Smaller nanoparticles can also be bound and assembled onto relatively larger nanoparticles as substrates and form dense ordered packing.[20,21]

Signal improvement in SERS measurements depends not only on the chemical and electromagnetic enhancement factors determined by the plasmonic properties of the SERS substrate but also on the number of molecules adsorbed and thus involved in the process, N_{SERS}. Plasmonic-magnetic particles have been used primarily in SERS-based immunoassay and detection of DNA for the capture of biomolecules, their extraction/concentration from a complex sample matrix, and measurement.[22−24] These properties also make plasmonic-magnetic nanoparticles attractive as a SERS substrate to concentrate chemical species from their dilute solutions and keep them proximate to the surface where the local EM field is effective. SERS is a powerful analytical technique due to its high structural selectivity and the capability of measuring Raman spectra from small sample volumes.[25,26] Integration of a one-step preconcentration process simply by utilizing plasmonic-magnetic bifunctional nanoparticles both as a solid phase sorbent and SERS substrate would improve the potency of this analytical technique for trace analysis.

Herein, $Co@SiO_2$ nanoparticles were used as a platform onto which AuNPs were attached for the first time. The prepared bifunctional $Co@SiO_2/AuNPs$ nanoparticles were applied both as a solid phase for magnetic collection in the preconcentration process and as SERS substrates for the detection of 4-mercaptobenzoic acid (4-MBA) amount. Consequently, the use of bifunctional $Co@SiO_2/AuNPs$ nanoparticles both for the collection of dissolved chemicals from the solution and for their SERS measurements is expected to bring an advantage from the quantitative analytical point of view.

2. Results and discussion

2.1. Preparation of gold nanoparticle-attached silica-coated cobalt nanoparticles

The morphology and particle sizes of the cobalt nanoparticles (CoNPs), gold nanoparticles (AuNPs), and bare $Co@SiO_2$ and $Co@SiO_2/AuNPs$ nanoparticles were examined with FE-SEM and TEM measurements. FE-SEM measurements were performed by using a QUANTA 400F field emission scanning electron microscope equipped with energy-dispersive X-ray (EDX) analyzer and TEM measurements were performed using an FEI 120-kV transmission electron microscope. The FE-SEM results of the CoNPs and TEM result of the AuNPs are given in Figures 1a and 1b, respectively.

The average dimensions of CoNPs and AuNPs were calculated as 46 ± 4 and 15 ± 3 nm, respectively. After that, FE-SEM measurements were performed to find the morphological properties of $Co@SiO_2$ and $Co@SiO_2/AuNPs$ nanoparticles and results are given in Figures 2a and 2b. Since the average dimensions of the AuNPs and $Co@SiO_2$ nanoparticles were around 15 ± 3 nm and 480 ± 32 nm, respectively, the FE-SEM images
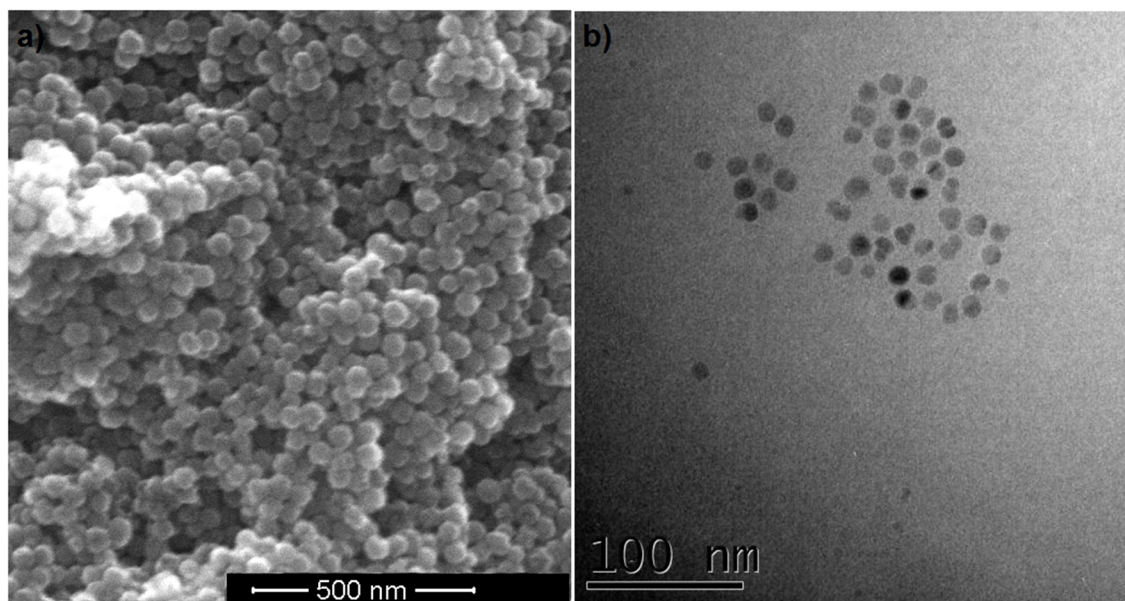
Figure 1. (a) FE-SEM images of CoNPs and (b) TEM image of AuNPs.

clearly show that AuNPs appear as spots on the silica surface and were deposited on the Co@SiO$_2$ surface. The AuNPs' deposition onto the Co@SiO$_2$ particles was also confirmed by EDX data as seen in Figures 2c and 2d. EDX analyses of randomly chosen nanoparticles clearly show the presence of Au besides the Co and Si used for the preparation of magnetic support.

2.2. Optical properties of gold nanoparticle-attached silica-coated cobalt nanoparticles

Attachment of AuNPs onto Co@SiO$_2$ was monitored by measuring plasmon absorption of AuNPs via following their UV-Vis absorption characteristics. UV-Vis spectra were collected over the range of 400–900 nm by using a double beam instrument (Varian Cary 100). The results are given in Figure 3.

As can be seen from Figure 3, the suspension of AuNPs used for attachment onto the surface of the magnetic Co@SiO$_2$ nanoparticles has peak absorption at 520 nm, whereas no spectral feature of Co@SiO$_2$ nanoparticles is observed in their UV-Vis spectra. However, when the AuNPs were added onto the Co@SiO$_2$ nanoparticle, an outer nanoparticulate Au layer was formed and the absorption maximum of the plasmon resonance excitation of the AuNPs appeared at 540 nm. The shift in the plasmon absorption band (520 nm) to longer wavelengths (540 nm) was attributed to the coupling between neighboring AuNPs on the surface.[27,28]

2.3. Effect of gold/cobalt-silica nanoparticle volume ratio on the density of gold nanoparticles attached onto silica-coated cobalt nanoparticles

The effect of Co@SiO$_2$/AuNPs volume ratio (v/v) on AuNPs' deposition on the surface of Co@SiO$_2$ nanoparticles was investigated in the volume ratio range of 0.1–4 by utilizing FE-SEM measurements, which are shown in Figures 4a–4f. AuNP deposition on the surface of Co@SiO$_2$ nanoparticles increases in accordance with the increase in AuNPs-Co@SiO$_2$ volume ratio (v/v) up to 2 in which AuNP was arranged in an ordered way on the surface and complete surface coverage was obtained. At higher volume ratios, deterioration was observed in the structure.
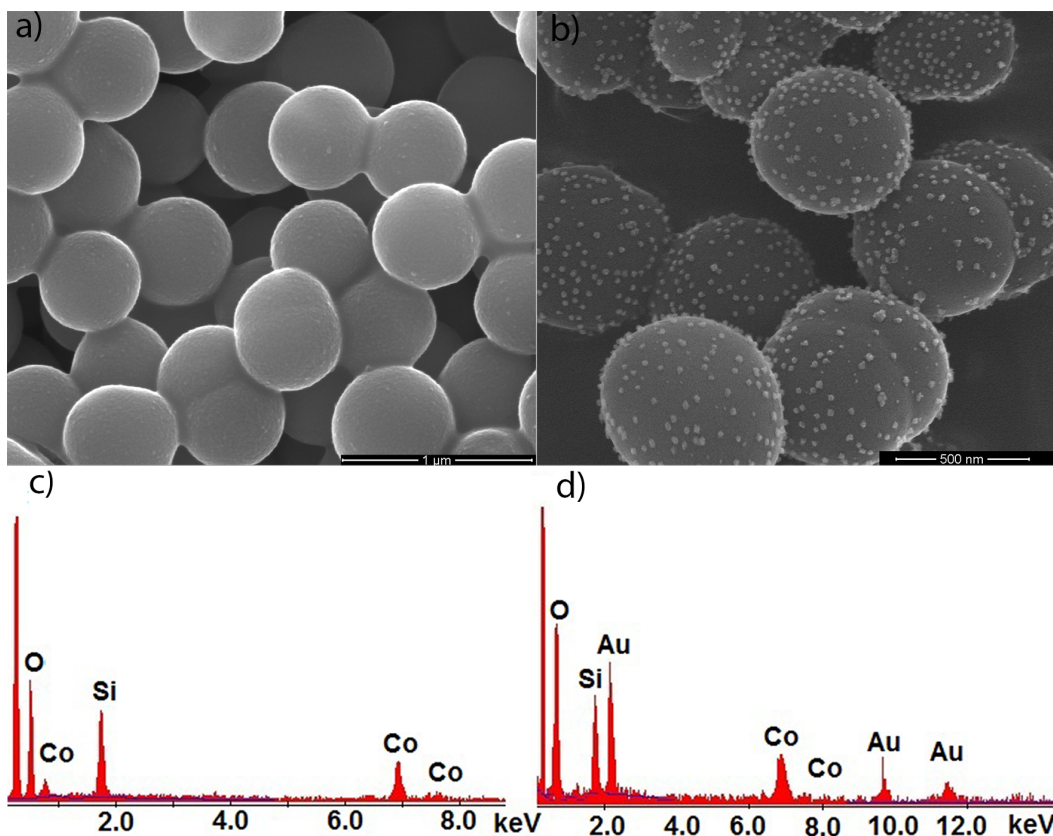
Figure 2. FE-SEM images of (a) Co@SiO$_2$ and (b) Co@SiO$_2$/AuNPs, and EDX patterns of (c) Co@SiO$_2$ and (d) Co@SiO$_2$/AuNPs.
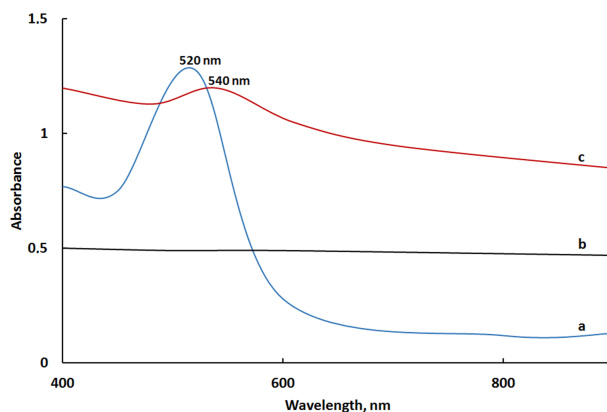

Figure 3. UV-Vis spectra of (a) AuNPs, (b) Co@SiO$_2$, and (c) Co@SiO$_2$/AuNPs nanoparticles.

Hence, a gold/cobalt-silica volume ratio of 2 was chosen as the optimum volume ratio and was used in further SERS applications.

2.4. Magnetic behavior of gold nanoparticle-attached silica-coated cobalt nanoparticles

Magnetic properties of the Co@SiO$_2$/AuNPs nanoparticles were characterized by using a vibrating sample magnetometer (VSM) at 300 K. Magnetic properties of the final structure were investigated with an ADE
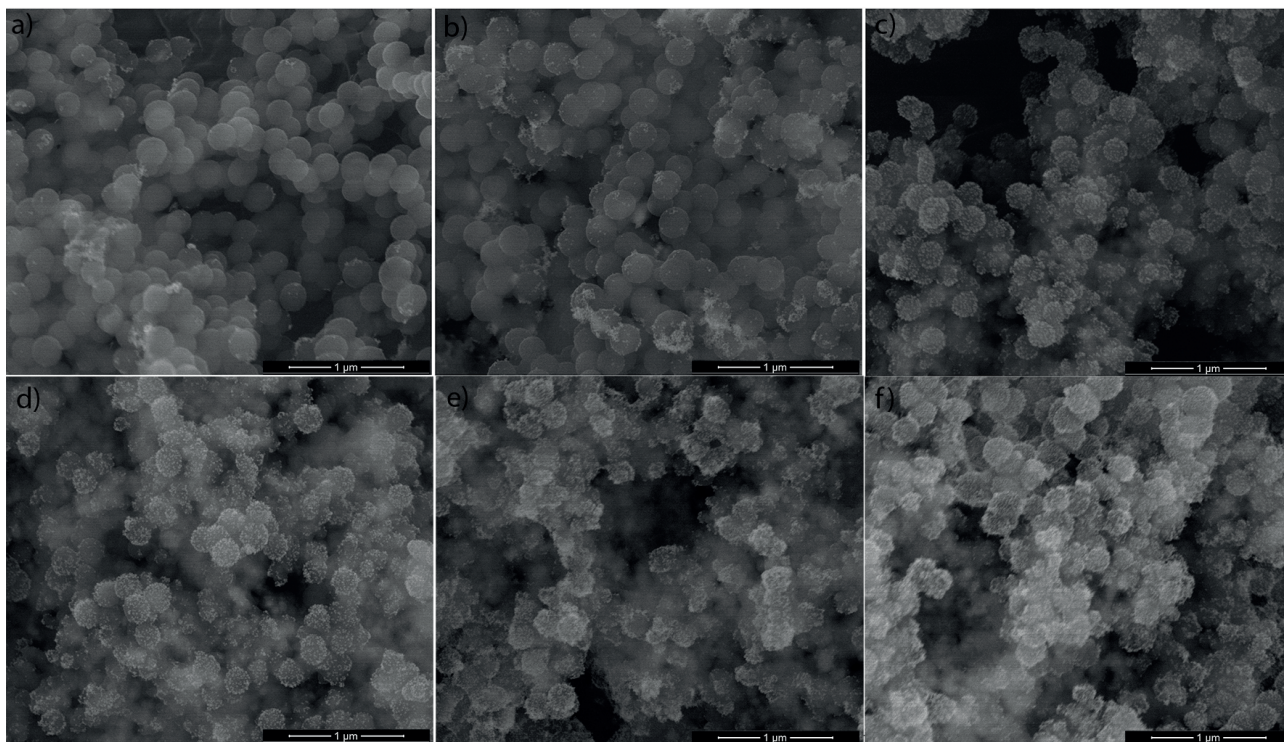
Figure 4. FE-SEM images of Co@SiO$_2$/AuNPs nanoparticles prepared at various AuNPs-Co@SiO$_2$ volume ratios (v/v): (a) 0.1, (b) 0.5, (c) 1, (d) 2 (e) 3, and (f) 4.

Model EV9 VSM having a maximum field of 2.2 T. A Nd$_2$Fe$_{14}$B magnet was used for magnetic separation applications. The saturation magnetization value was founded as 15 emu/g by considering the total weight of the composites. The coercivity value was measured as 16.154 Oe for Co@SiO$_2$/AuNPs nanoparticles. Because of their magnetic characteristics, the prepared nanoparticles can be collected from their dispersions by using an external magnet. This property is clearly seen in photographs given in Figures 5a and 5b. As can be seen from Figure 5a, the color of the nanocomposite dispersion was dark red-violet. After the application of an external magnetic field, nanocomposites dispersed in solution were collected, and a clear dispersion medium was obtained, as shown in Figure 5b. Collected nanoparticles can be redispersed after the removal of the external magnetic field.

2.5. The performance of gold nanoparticle-attached silica-coated cobalt nanoparticles as SERS substrate

Co@SiO$_2$/AuNPs nanoparticles are thought to be useful as SERS substrates as the AuNPs are closely spaced, the roughness is determined by the size of the particles, and the coverage seems to be uniform. Their performance as SERS substrates was evaluated initially by using BCB and R6G as model compounds. For SERS measurements a Jobin Yvon LabRam confocal microscopy Raman spectrometer equipped with 1800 grooves/mm grating and 20 mW He-Ne laser with 632.8 nm radiation was used. Upon addition of BCB and R6G, with a final concentration of 1×10^{-7} M and 1×10^{-6} M, respectively, onto Co@SiO$_2$/AuNPs nanoparticles, SERS spectra were collected. Typical SERS spectra of BCB and R6G adsorbed on Co@SiO$_2$/AuNPs nanoparticles are shown in Figures 6a and 6b.
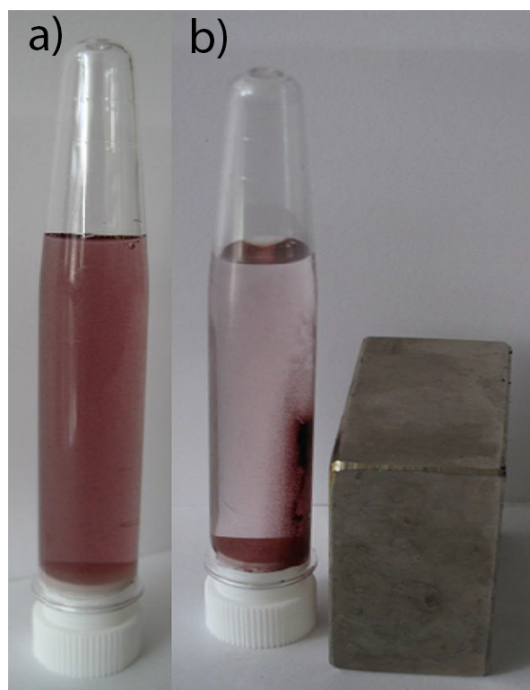
Figure 5. Photograph of a suspension of Co@SiO$_2$/AuNPs nanoparticles in the absence (a) and presence (b) of an external magnetic field.
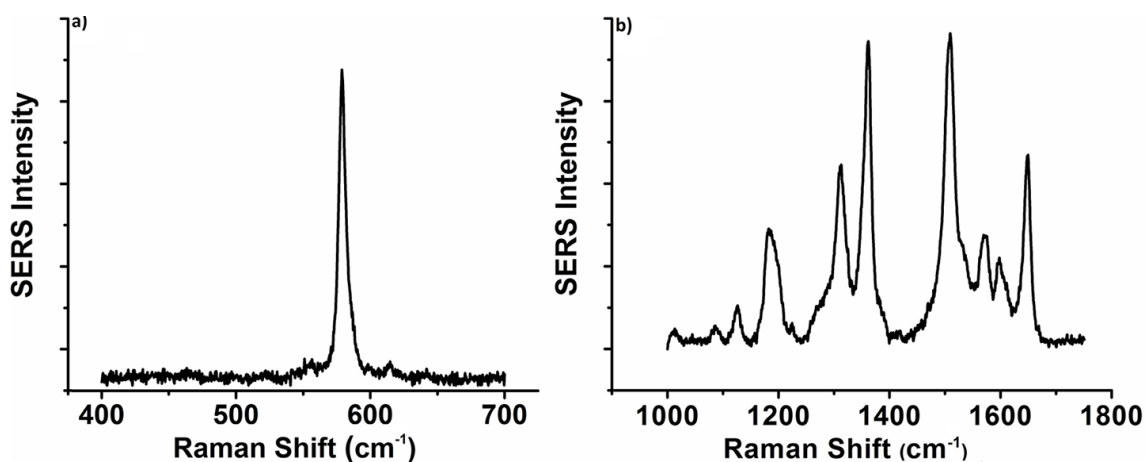
Figure 6. SERS signal of (a) 1×10^{-7} M BCB and (b) 1×10^{-6} M R6G obtained with Co@SiO$_2$/AuNPs substrate with 10 s of integration of 632.8 nm, 20 mW He-Ne laser.

In the SERS spectrum of BCB (Figure 6a), the intense band around 580 cm^{-1} is related to the benzene ring deformation mode. In the case of R6G (Figure 6b), the peak at about 1188 cm^{-1} is related to the C-C stretching vibrations. The intense peaks at 1303, 1356, and 1575 cm^{-1} are correlated with the aromatic C-C stretching vibrations.[29]

After that, the effect of AuNP amount on the SERS intensity was investigated by using Co@SiO$_2$/AuNPs prepared with the different AuNPs-Co@SiO$_2$ volume ratios given in Figure 4. For this, SERS measurements of 1×10^{-7} M BCB were performed by using prepared substrates. Results are given in Figure 7.
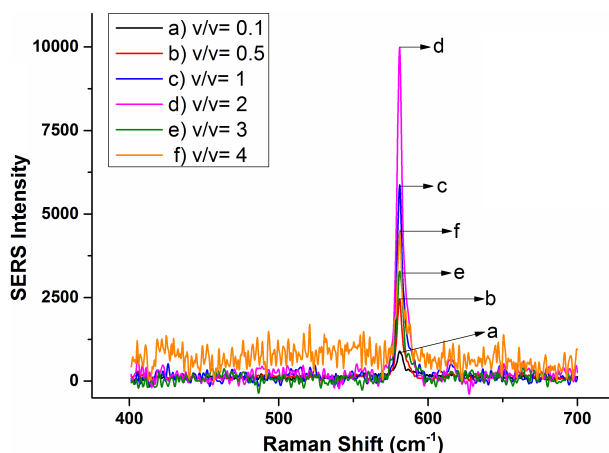
Figure 7. SERS signal of 1×10^{-7} M BCB obtained with $Co@SiO_2$/AuNPs substrate prepared with different AuNPs-$Co@SiO_2$ volume ratios (v/v): (a) 0.1, (b) 0.5, (c) 1, (d) 2 (e) 3, and (f) 4 under 10 s of integration of 632.8 nm, 20 mW He-Ne laser.

According to the obtained results, as the amount of AuNPs increases, the SERS intensity of BCB increases until the point of AuNPs-$Co@SiO_2$ volume ratio (v/v) of 2. At higher concentrations, SERS intensities decrease due to the loss in uniformity of surface and hot spot points. The obtained results are consistent with the results given in Figure 4.

In order to show the batch-to-batch reproducibility (RSD%) of the SERS measurements, 4 different SERS substrates were prepared and used for the measurement of 1×10^{-7} M BCB. The results are given in Figure 8.
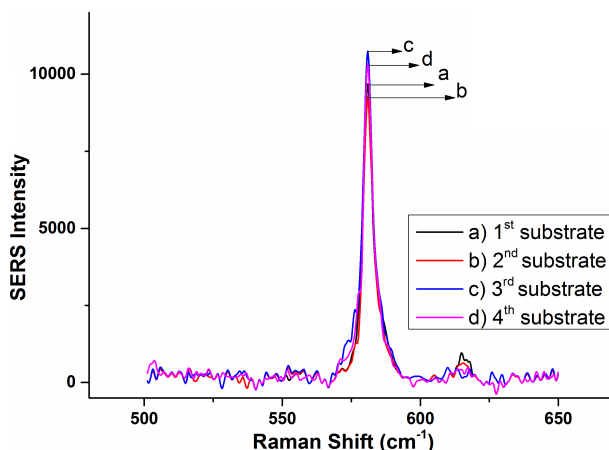
Figure 8. SERS spectra of 10^{-7} M BCB acquired at four different substrates prepared with $Co@SiO_2$/AuNPs.

The RSD% of the SERS spectra on the same substrate was calculated as 6.9% by taking the average and standard deviation of the peak intensities at around 580 cm^{-1} for these four SERS spectra.

Finally, the enhancement power of the prepared substrate was also compared with the one prepared with silver nanoparticles (AgNPs), known as the most common SERS substrate material. The FE-SEM images of the structures used as SERS substrates are given in Figures 9a and 9b. Obtained SERS spectra are given in Figure 9c.

As is known, generally AgNPs exhibit higher SERS enhancement (at least twofold) at 632 nm laser
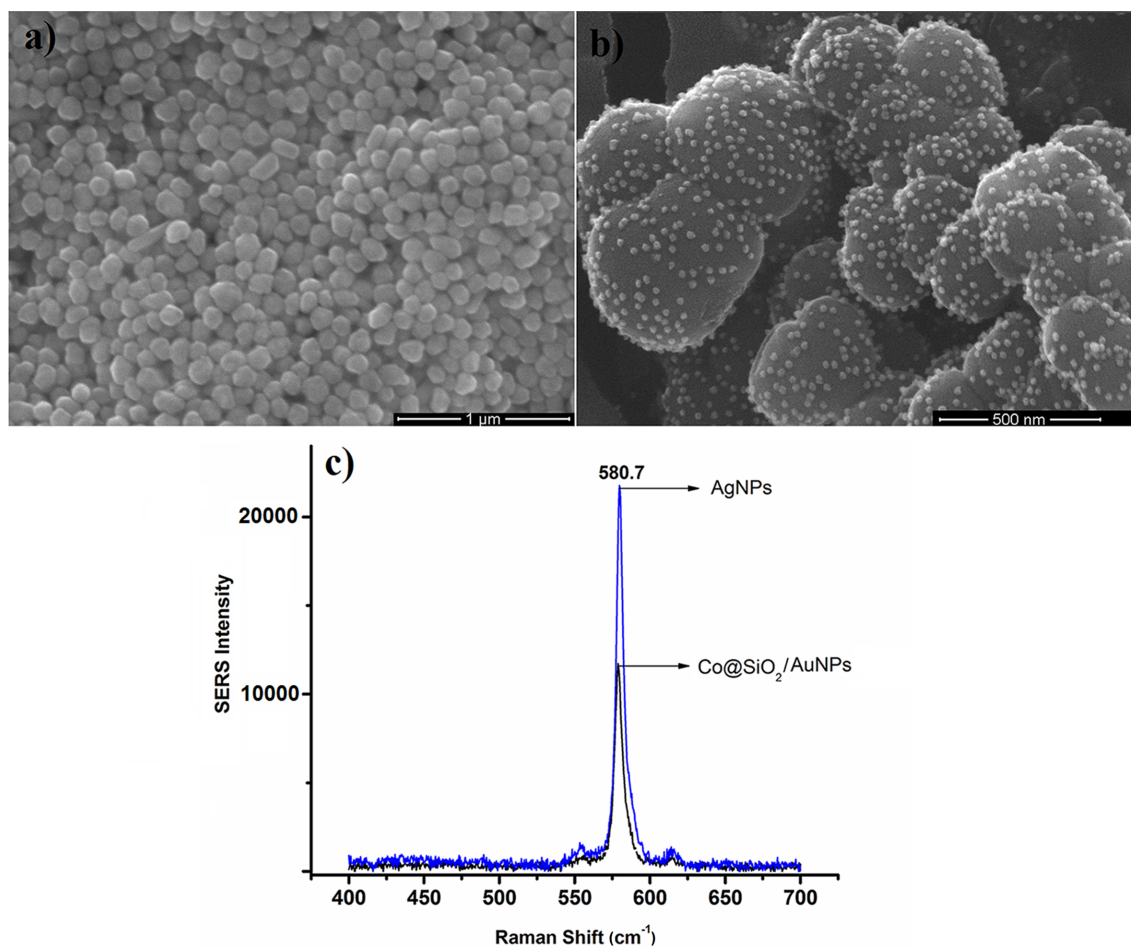
Figure 9. FE-SEM images of (a) AgNP and (b) Co@SiO$_2$/AuNPs nanoparticles and (c) comparison of SERS signal of 1×10^{-7} M BCB obtained with Co@SiO$_2$/AuNPs and AgNPs substrate.

irradiation when compared with AuNPs.[30] As can be seen from the Figure 9c, the performance of prepared particles as SERS substrate is comparable with the AgNPs due to hot spots generated. Therefore, considering the higher stability of AuNPs and comparable enhancement factor with AgNPs besides the preconcentration property, Co@SiO$_2$/AuNPs can be a good candidate for the SERS measurements of important molecules.

2.6. Performance of gold nanoparticle-attached silica-coated cobalt nanoparticles both as magnetic separation units and SERS substrate for preconcentration and detection of 4-MBA

Thiol-containing compounds are known to exhibit high reactivity toward gold nanoparticles, which results in the displacement of the citrate shell by the thiolate shell.[31] The reactivity, due to the affinity of thiol groups to gold, was exploited as an effective mean for SERS detection of 4-MBA in which the Co@SiO$_2$/AuNPs nanoparticles act as substrates. The results are given in Figure 10. Characteristic peaks, corresponding to v(C-C) ring-breathing modes (1078 and 1585 cm^{-1}), δ(C-H) (1173 cm^{-1}) and v_s (COO$^-$) (1423 cm^{-1}) modes were observed in SERS spectra of 4-MBA. The band at 1423 cm^{-1} with a wide shoulder below 1400 cm^{-1} was assigned to the nonbonded COO$^-$ groups and it was concluded that the appearance of this band in the SERS spectrum of 4-MBA could indicate more vertically oriented molecules.[32,33] In the SERS measurements

equal volumes (100 µL) of the sample and substrate were mixed and 15 µL of the mixture was used for a single measurement. The limit of detection (3s) for 4-MBA by using $Co@SiO_2/AuNPs$ nanoparticles as SERS substrate was estimated to be 2.5×10^{-5} M.

When the 4-MBA concentration was lowered to 1×10^{-5} M, no SERS signal was observed with $Co@SiO_2/AuNPs$ nanoparticles, as expected. In order to be able to improve the sensitivity of the SERS measurement and lower the detection limit by increasing N_{SERS}, the volume of the sample was increased while keeping the aliquot size of the $Co@SiO_2/AuNPs$ nanoparticles small. In a typical experiment, 1 mL of $Co@SiO_2/AuNPs$ nanoparticles dispersion taken from stock suspension (0.2 mg/mL) was added into 5 mL of 1×10^{-5} M 4-MBA solution (the final concentration of 4-MBA was 8.3×10^{-6} M). Following 10 min of batch-type solid phase extraction, particles were collected by external magnetic field and redispersed in 200 µL of water. The SERS spectrum of 15 µL of this nanodispersion was acquired directly for the quantification of 4-MBA (Figure 10). As can be seen from Figure 10, all of the peaks corresponding to 4-MBA are enhanced.
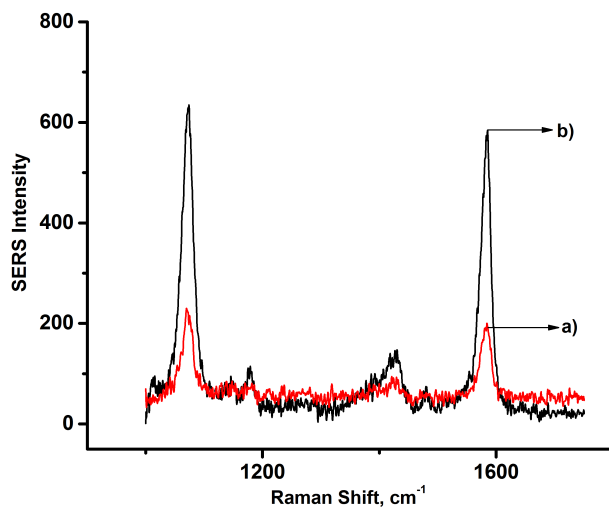
Figure 10. SERS spectrum of (a) 1×10^{-4} M 4-MBA taken with $Co@SiO_2/AuNPs$ substrate directly, without extraction, and (b) 8.3×10^{-6} M 4-MBA taken with $Co@SiO_2/AuNPs$ substrate after solid phase extraction with 10 s of integration of 632.8 nm, 20 mW He-Ne laser.

The SERS signal of 8.3×10^{-6} M 4-MBA collected on the surface of $Co@SiO_2/AuNPs$ magnetic nanoparticles after magnetic separation is almost five times higher than that of the 1×10^{-4} M 4-MBA measured without preconcentration. Comparisons are based on the aromatic ring vibration mode at 1594 cm^{-1}.[34] The enhancement on SERS signal intensity was attributed to the effective assembling of 4-MBA onto the $Co@SiO_2/AuNPs$ particles throughout the equilibration in a comparatively larger volume of the lower concentration of 4-MBA solution, such as 1.0×10^{-5} M. It is well known that SERS is a distance-dependent phenomenon; hence, the surface coverage of analyte molecules onto the SERS active nanoparticles is predominantly important in the signal enhancement. Therefore, the solid phase affinity extraction of the analyte, through a magnetic separation and the measurement of the SERS signal on the same magnetic particles without elution, brings the advantages of high sensitivity and low detection limit to SERS studies. In such an application, the magnetic and plasmonic properties of the nanoparticles, their stability, and size homogeneity are the important parameters. The prepared $Co@SiO_2/AuNPs$ magnetic-plasmonic bifunctional nanoparticles satisfy all the conditions, and approximately 50-fold increase in SERS intensity was achieved through solid-phase

extraction of 4-MBA using Co@SiO$_2$/AuNPs nanoparticles in 10 min. Relative standard deviation for the results of replicate measurements was below 8.0%. Larger sample volumes will lead to obtaining lower detection limits. If it becomes difficult to collect the magnetic nanoparticles with a small magnet from a large sample volume, then the sample volume can be kept at a convenient level, but aliquot size of the Co@SiO$_2$/AuNPs nanoparticles can be decreased and collected in a smaller volume.

2.7. Conclusions

The magnetic and optical bifunctional nanoparticles produced in this study offer unique advantages over the other available substrates in SERS measurements. They can be utilized both as suspension and as solid support on slides. While the surface plasmons of AuNPs attached to the magnetic nanoparticles give efficient SERS capabilities, the magnetic property provides the quick separation of analytes from the mixture. The AuNP layer attracts the analytes particularly having thiol groups and amplifies their SERS responses. By using Co@SiO$_2$/AuNPs nanoparticles for sample preconcentration and SERS measurement, we have accomplished 50-fold signal ampli?cation of 4-MBA with an additional potential to improve the sensitivity and detection limit. Enhancement factor can be increased by using larger sample volumes. In its application to natural samples, any molecules containing a thiol group might be attracted to the gold surface, preconcentrated, and could be determined owing to their characteristic SERS spectra. Therefore, the use of this nanotechnology-based bifunctional substrate can open a road for easy and efficient analysis in various matrices.

3. Experimental

3.1. Preparation of amine-functionalized silica-coated cobalt nanoparticles

In order to prepare cobalt nanoparticles (CoNPs), initially N$_2$ was passed through 20 mL of distilled water containing 2 mL (1%) of trisodium citrate solution.[35] After that the solution was transfer into a 3-necked round-bottom flask and stirred under N$_2$ atmosphere. Then 0.2 mL of 0.4 M CoCl$_2$.6H$_2$O solution was added to the solution, and reduction was performed with the addition of NaBH$_4$. The concentration of obtained CoNPs was calculated as 2.25×10^{-12} mol/dm^3. After a black-colored solution was obtained, CoNPs were coated with a silica layer by using the Stöber method for protection against air oxidation and further functionalization.[36] For this, 80 mL of ethanol containing 17.0 µL of tetraethyl orthosilicate (TEOS) and 1.44 µL of 3-aminopropyltrimethoxysilane (APTMS) were added and the solution was further stirred for 3 h. For the addition of amine groups onto the silica-coated nanoparticles, 6 µL of 3-aminopropyltriethoxysilane (APTES) was added to the CoNPs-alcoholic TEOS mixture and stirred for 12 h. Then the particles were collected by using an external magnet, washed with ethanol and water, and dried. Finally, 30 mg of prepared particles were dispersed in 100 mL of water (0.3 mg/mL) and used as stock suspension for further studies.

3.2. Preparation of gold-assembled silica-coated cobalt nanoparticles

AuNPs were prepared according to the citrate reduction method.[27] An aqueous solution containing 144 µL of HAuCl$_4$ (0.1 M), in a 50-mL beaker, was stirred and heated. When boiling started, 2 mL of 1% (w/v) trisodium citrate solution was added to the solution. Then the solution was stirred vigorously and boiled for 1 h. After that, it was allowed to cool to room temperature by continuous stirring. Then 5 mL of amine-modified Co@SiO$_2$ magnetic nanoparticle taken from the stock suspension (0.3 mg/mL) was sonicated for 5 min to prevent aggregation before the treatment with AuNPs. This dispersion was mixed with 10 mL of citrate-

stabilized AuNPs with a concentration of 4.0×10^{-14} mol/dm^3 and vigorously stirred. Excess AuNPs were removed by repeated magnetic collection/wash cycles and finally the collected Co@SiO$_2$/AuNPs were dried and 2 mg of particles was redispersed in 10 mL of water (0.2 mg/mL).

3.3. Magnetic collection and SERS identification studies

Initially the enhancement power of the prepared SERS substrate was investigated. For the SERS measurements 100 µL of Co@SiO$_2$/AuNPs nanoparticles dispersion taken from 0.2 mg/mL stock suspension was mixed with the same volume of Raman indicator molecules and vortexed. Then 15 µL of the resulting mixture was dropped onto a glass slide and SERS measurements were carried out in the range of 400–800 cm^{-1} for BCB and 1000–1800 cm^{-1} for R6G. For preconcentration and identification of 4-MBA, 1 mL of Co@SiO$_2$/AuNPs nanoparticles dispersion taken from 0.2 mg/mL stock suspension and 5 mL of 1×10^{-5} M 4-MBA solution were added to a test tube. The final concentration of 4-MBA was 8.3×10^{-6} M. The test tube was shaken horizontally for 10 min and then the supernatant was removed by magnetic decantation process. Following preconcentration, magnetically collected particles were dispersed in 200 µL of water. For SERS measurements, 15 µL of this dispersion was placed on a glass slide and SERS measurements were performed within a range of 1000–2000 cm^{-1} by utilizing a Jobin Yvon LabRam confocal microscopy Raman spectrometer equipped with 1800 grooves/mm grating and 20 mW, 632.8 nm He-Ne laser.

Acknowledgment

References

1. Shuaidi, Z.; Geryak, R.; Geldmeier, J.; Kim, S.; Tsukruk, V. V. *Chem. Rev.* **2017**, *117*, 12942-13038.

2. Li, M.; Luo, Z.; Zhao, Y. *Chem. Mater.* **2018**, *30*, 25-53.

3. Costi, R.; Saunders, A. E.; Banin, U. *Angew. Chem. Int. Edit.* **2010**, *49*, 4878-4897.

4. Xu, Z.; Hou, Y.; Sun, S. *J. Am. Chem. Soc.* **2007**, *129*, 8698-8699.

5. Materia, M. E.; Leal, M. P.; Scotto, M., Balakrishnan, P. B.; Avugadda, S. K.; García-Martín, M. L.; Cohen, B. E.; Chan, E. M.; Pellegrino, T. *Bioconjugate Chem.* **2017**, *28*, 2707-2714.

6. Shi, B.; Du, X.; Chen, J.; Fu, L.; Morsch, M.; Lee, A.; Liu, Y.; Cole, N.; Chung, R. *Small* **2017**, *13*, 1603966.

7. Larsen, G. K.; Farr, W.; Murph, S. E. H. *J. Phys. Chem. C* **2016**, *120*, 15162-15172.

8. Nasir Baig, R. B.; Varma, R. S. *Green Chem.* **2012**, *14*, 625-632.

9. Lai, H.; Xu, F.; Wang, L. *J. Mater. Sci.* **2018**, *53*, 8677-8698.

10. Jun, B. H.; Noh, M. S.; Kim, J.; Kim, G.; Kang, H.; Kim, M. S.; Seo, Y. T.; Baek, J.; Kim, J. H. *Small* **2010**, *6*, 119-125.

11. Du, J.; Jing, C. *J. Phys. Chem. C* **2011**, *115*, 17829-17835.

12. Stiles, P. L.; Dieringer, J. A.; Shah, N. C.; Van Duyne, R. R. *Annu. Rev. Anal. Chem.* **2008**, *1*, 601-626.

13. Banholzer, M. J.; Millstone, J. E.; Qin, L.; Mirkin, C. A. *Chem. Soc. Rev.* **2008**, *37*, 885-897.

14. Eustis, S.; El-Sayed, M. A. *Chem. Soc. Rev.* **2006**, *35*, 209-217.

15. Jeon, T. Y.; Park, S. G.; Lee, S. Y.; Jeon, H. C.; Yang, S. M. *ACS Appl. Mater. Inter.* **2013**, *5*, 243-248.

16. Hoon Kim, N.; Hwang, W.; Baek, K.; Rohman, M. R.; Kim, J.; Kim, H. W.; Mun, J.; Lee, S. Y.; Yun, G.; Murray, J. et al. *J. Am. Chem. Soc.* **2018**, *140*, 4705-4711.

17. Herzog, J. B.; Knight, M. W.; Li, Y.; Evans, K. M.; Halas, N. J.; Natelson, D. *Nano Lett.* **2013**, *13*, 1359-1364.

18. Liz-Marzain, L. M. *Langmuir* **2006**, *22*, 32-41.

19. Daniel, M. C.; Astruc, D. *Chem. Rev.* **2004**, *104*, 293-346.

20. Fana, M.; Andradec, G. F. S.; Brolod, A. G. *Anal. Chim. Acta.* **2011**, *693*, 7-25.

21. Muhlig, S.; Cunningham, A.; Scheeler, S.; Pacholski, C.; Burgi, T.; Rockstuhl, C.; Lederer, F. *ACS Nano* **2011**, *5*, 6586-6592.

22. Wang, H.; Brandl, D. W.; Fei, L., Nordlander, P.; Halas, N. *Nano Lett.* **2006**, *6*, 827-832.

23. Bao, F.; Yao, J. L.; Gu, R. A. *Langmuir* **2009**, *25*, 10782-10787.

24. Tamer, U.; Boyaci, I. H.; Temur, E.; Zengin, A.; Dincer, I.; Erman, Y. *J. Nanopart. Res.* **2011**, *13*, 3167-3176.

25. Zhang H.; Harpster, M. H.; Wilson, W. C.; Johnson, P. A. *Langmuir* **2012**, *28*, 4030-4037.

26. Qian, X. M.; Nie, S. M. *Chem. Soc. Rev.* **2008**, *37*, 912-920.

27. Enustun, B. V.; Turkevich, J. *J. Am. Chem. Soc.* **1963**, *8*, 3317-3328.

28. Caruso, F.; Spasova, M.; Salgueirino-Maceira, V.; Liz-Marzan L. M. *Adv. Mater.* **2001**, *13*, 1090-1094.

29. Salgueirino-Maceira,V.; Caruso, F.; Liz-Marzan, L. M. *J. Phys. Chem. B* **2003**, *107*, 10990-10994.

30. Schatz, G. C.; Van Duyne, R. P. In *Handbook of Vibrational Spectroscopy*, Chalmers, J. M; Griffiths, P. R., Eds. Wiley: New York, NY, USA, 2002, pp. 759-774.

31. Schmid, T.; Zhang, W.; Zenobi, R. *Anal. Bioanal. Chem.* **2007**, *38*, 2655-2662.

32. Zhang, F. X.; Han, L.; Israel, L. B.; Daras, J. G.; Maye, M. M.; Ly, N. K.; Zhong, C. J. *Analyst* **2002**, *127*, 462-465.

33. Michota, A.; Bukowska, J. *J. Raman. Spectrosc.* **2003**, *34*, 21-25.

34. Orendorff, C. J.; Gole, A.; Sau, T. K.; Murphy C. J. *Anal. Chem.* **2005**, *77*, 3261-3266.

35. Schwartzberg, A. M.; Olson, T. Y.; Talley, C. E.; Zhang, J. Z. *J. Phys. Chem. B* **2006**, *110*, 19935-19944.

36. Stober, W.; Fink, A.; Bohn, E. *J. Colloid Interf. Sci.* **1968**, *26*, 62-69.